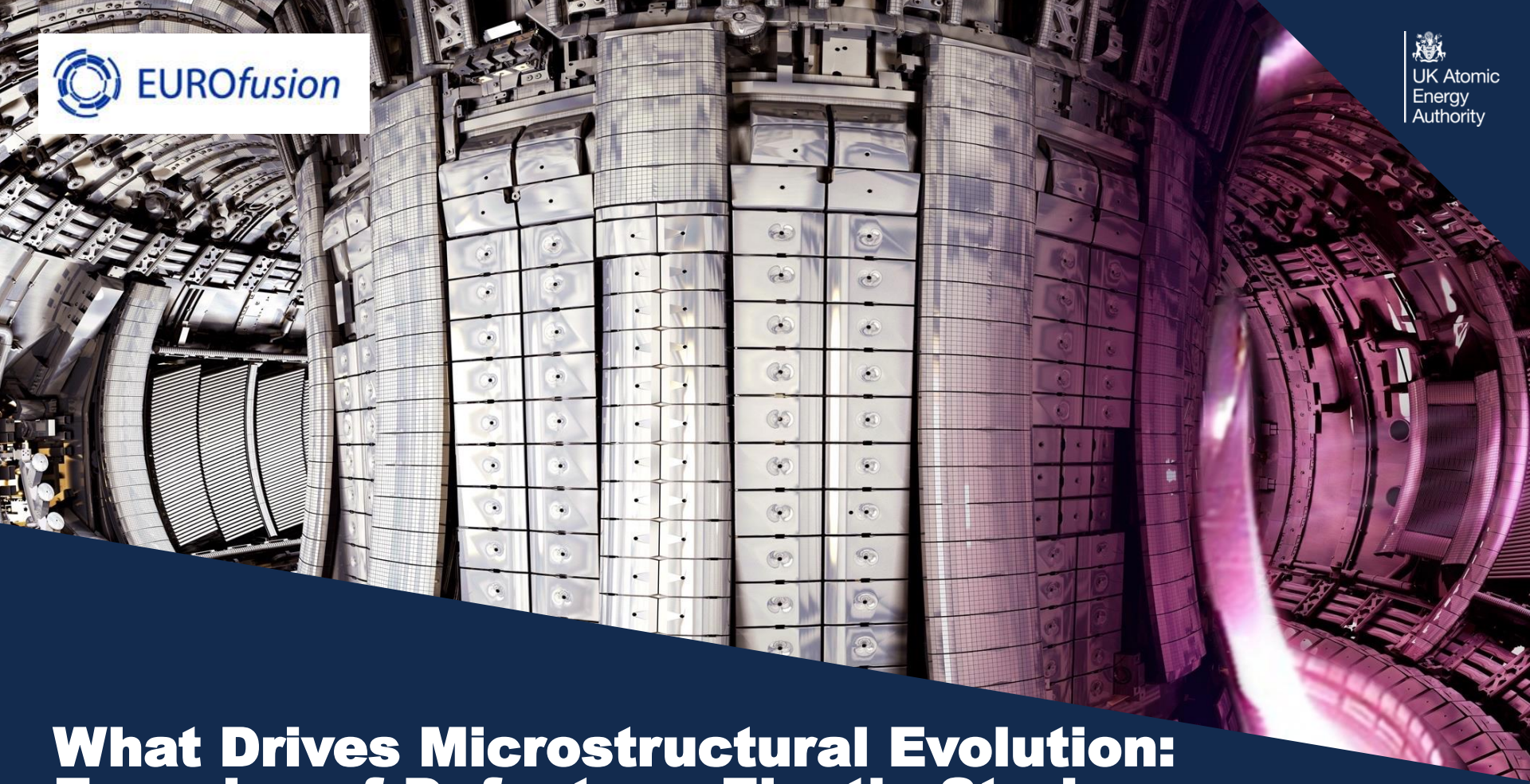

What Drives Microstructural Evolution: Energies of Defects or Elastic Strains and Stresses?

S.L. Dudarev, P.-W. Ma, D.R. Mason, and F. Hofmann

UK Atomic Energy Authority, Culham Centre for Fusion Energy, Oxfordshire, UK
Department of Engineering, University of Oxford, Parks Road, Oxford OX1 3PJ, UK


JET tokamak

UK Atomic Energy Authority

ITER

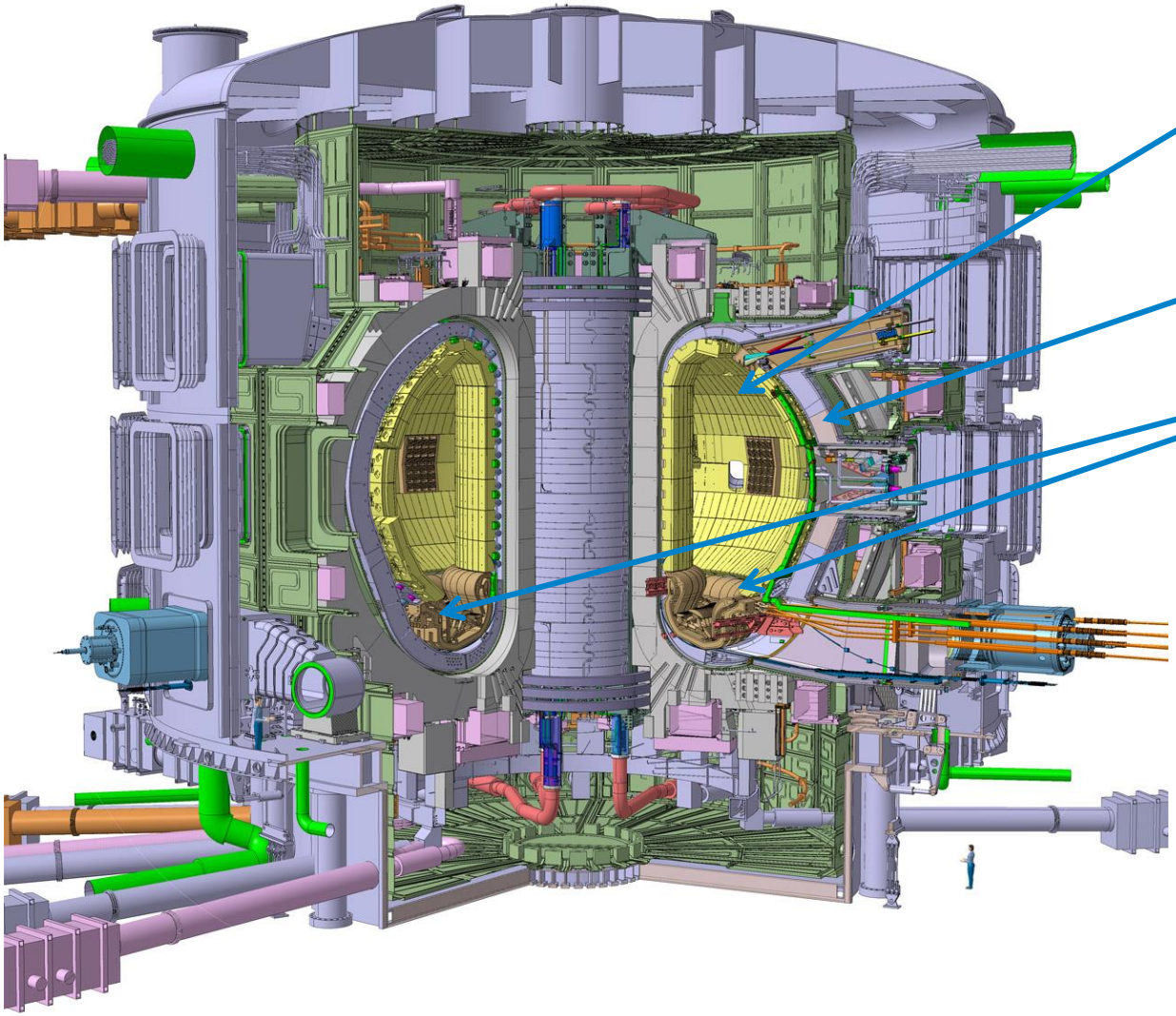

Plasma-facing tiles (beryllium)

Tritium breeding blanket modules (FM steel)

Divertor (tungsten +CuCrZr)

JET

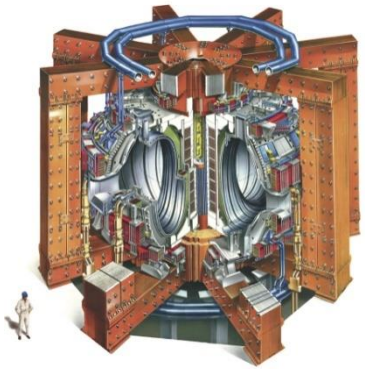

Fusion experiments: scaling up

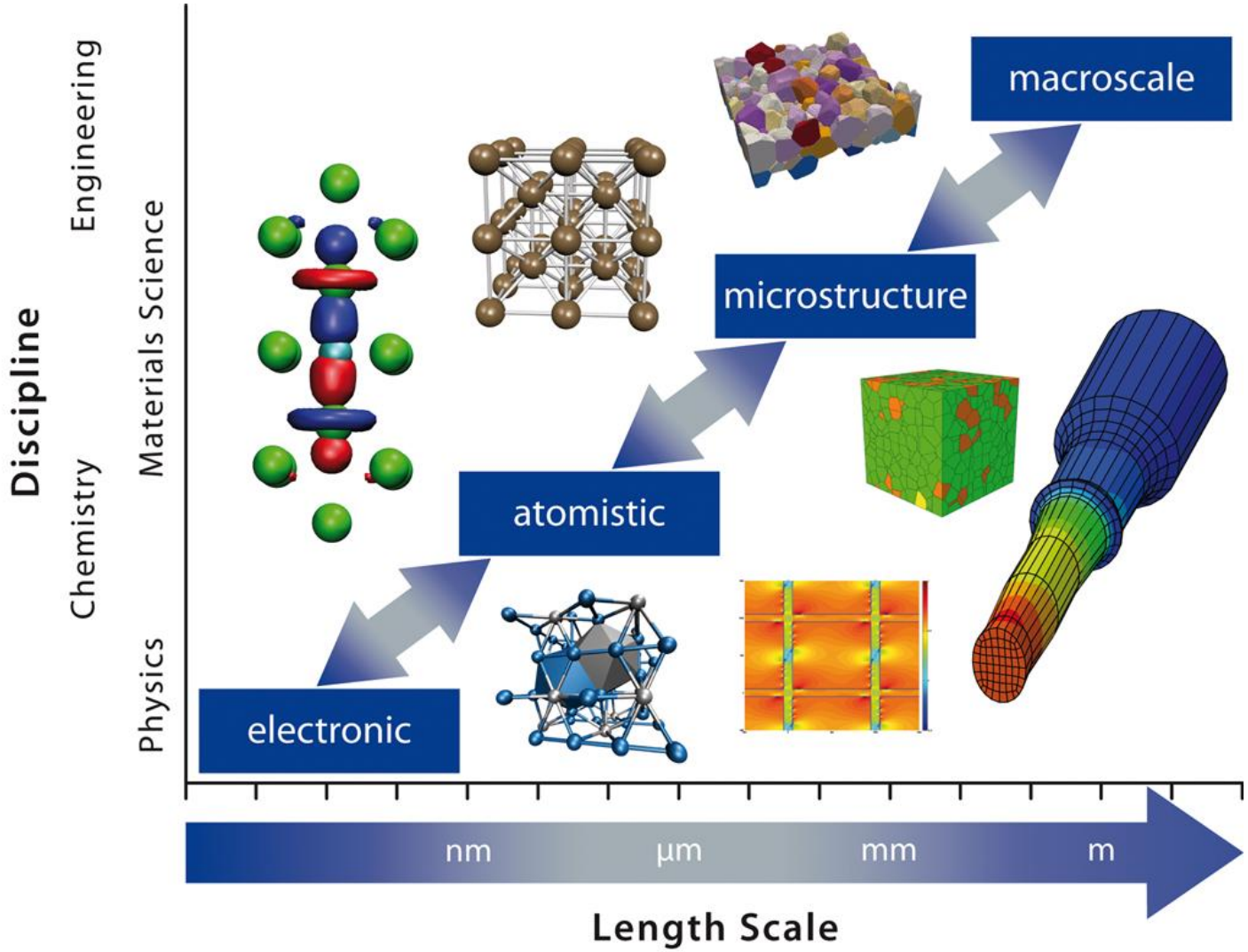

Hierarchical multiscale modelling – a conventional way to macroscale simulations.

The structure of elementary defects

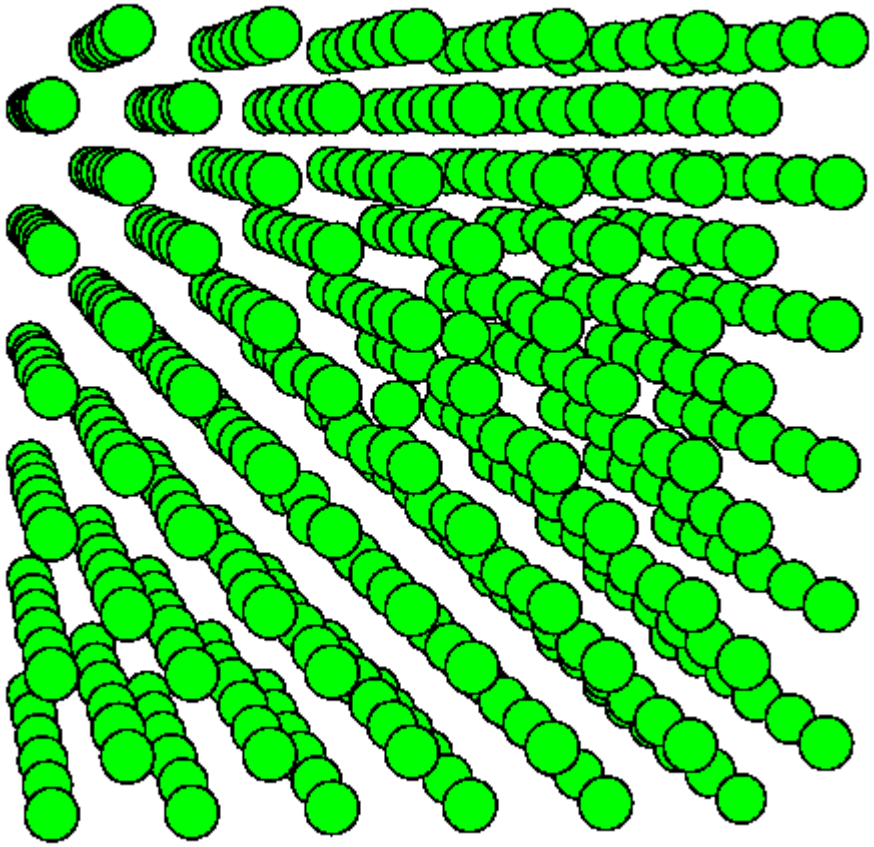

A self-interstitial atom defect in body-centred cubic (bcc) iron.

The structure of elementary defects

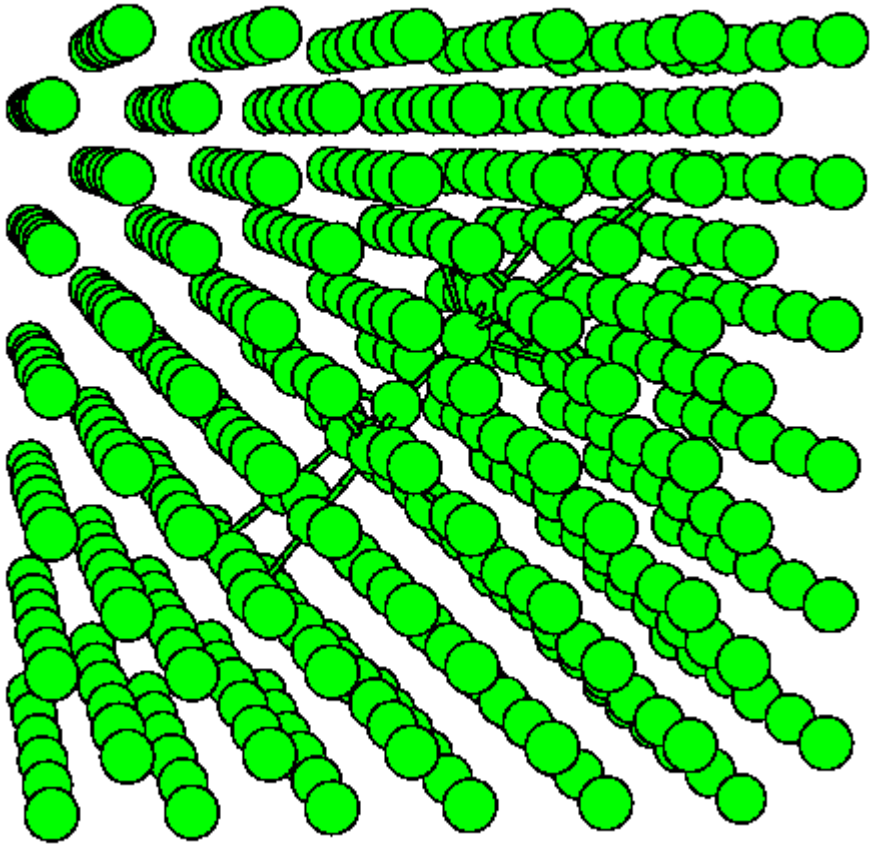

A self-interstitial atom defect in body-centred cubic (bcc) iron.

The structure of elementary defects

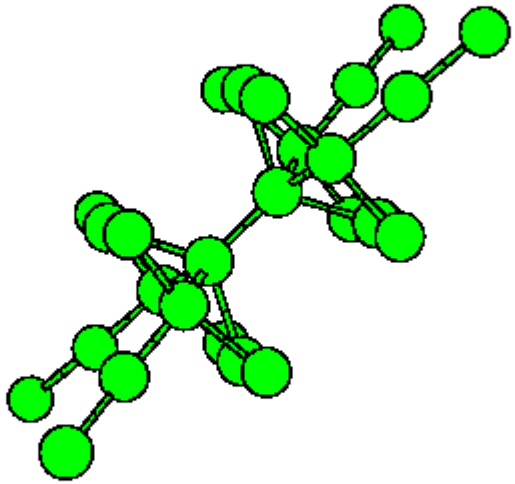

A self-interstitial atom defect in body-centred cubic (bcc) iron.

Formation and migration energies

UK Atomic Energy Authority

	⟨111⟩	⟨110⟩	⟨100⟩	Tetrahedral	Octahedral	E_m
Fe	4.66,[b] 4.45[c]	3.94,[b] 3.75[c]	5.04,[b] 4.75[c]	4.26[c]	4.94[c]	0.34[c]
V	3.37,[d] 3.14[e]	3.65,[d] 3.48[e]	3.92,[d] 3.57[e]	3.84,[d] 3.69[e]	3.96,[d] 3.62[e]	
Nb	5.25[d]	5.60[d]	5.95[d]	5.76[d]	6.06[d]	
Ta	5.83[d]	6.38[d]	7.00[d]	6.77[d]	7.10[d]	
Cr	5.66[d]	5.68[d]	6.64[d]	6.19[d]	6.72[d]	
Mo	7.42,[d] 7.34[e]	7.58,[d] 7.51[e]	9.00,[d] 8.77[e]	8.40,[d] 8.20[e]	9.07,[d] 8.86[e]	
W	9.55[d]	9.84[d]	11.49[d]	11.05[d]	11.68[d]	
Al	1.959[f]	1.869[f]	1.579[f]	1.790[f]	1.978[f]	0.084[f]
Ni	4.69[g]	4.99[g]	4.07[g]	4.69[g]	4.25[g]	0.14[g]
Si	3.84[h]	3.80 (hexagonal)	3.85 (caged)	4.07[h]	4.8	0.18[h]

	Al	Cu	Au	Ni	Pd	Pt	Pu
E_f	0.580[i]	1.04[d]	0.782[i]	1.37,[e] 1.43,[r] 1.65[r]	1.70[j]	1.18[j]	1.31, 1.36, 1.08[t]
E_m	0.57[m]	0.72[d]	–	1.285,[e] 1.08[r]	–	1.51[j]	–
	V	**Nb**	**Ta**	**Cr**	**Mo**	**W**	**Fe**
E_f	2.51[l]	2.99[l]	3.14[l]	2.64[l]	2.96,[j] 2.96[l]	3.56[l]	2.02,[b] 2.07,[k] 2.15[l]
E_m	0.62[l]	0.91[l]	1.48[l]	0.91[l]	1.28[l]	1.78[l]	0.65,[b] 0.67,[k] 0.64[l]
	C	**Si**	**Ge**	**Be**	**Ti**	**Zr**	**Hf**
E_f	8.2[f]	3.17,[c] 3.29[g]	2.3[h]	0.81,[n] 1.09[o]	1.97,[p] 2.13[q]	2.17,[q] 1.86[s]	2.22[q]
E_m	1.7[f]	0.4[g]	–	0.72B, 0.89NB[o]	0.47B, 0.61NB[p]	0.51B, 0.67NB[q]	0.79B, 0.91NB[q]

Annual Review of Materials Research 43 (2013) 35

Structure of self-interstitial defects

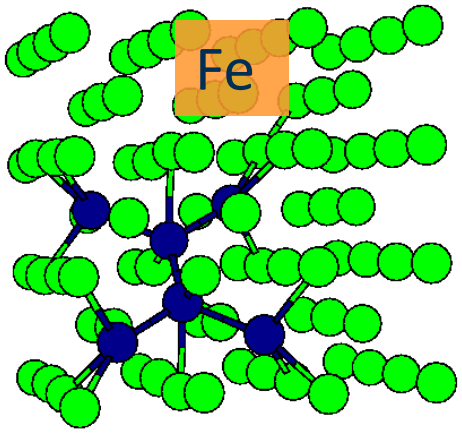

110 dumbbell

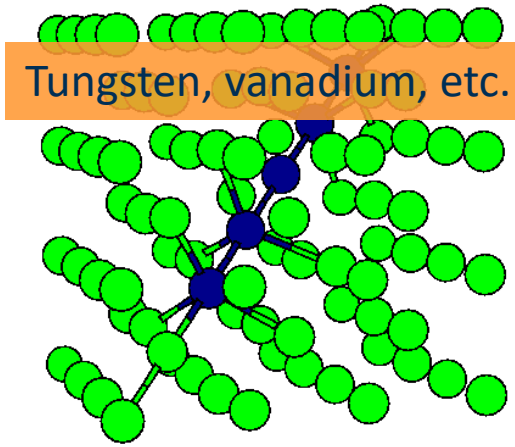

111 crowdion

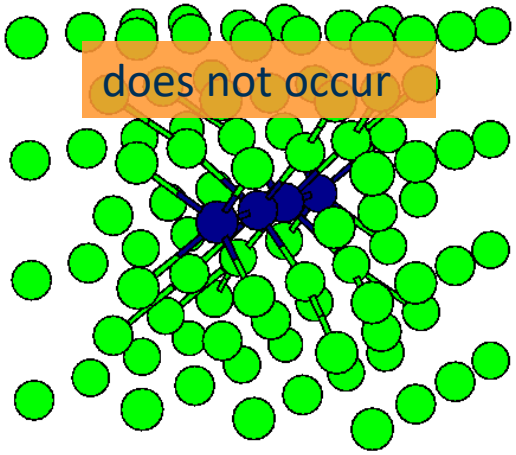

100 crowdion

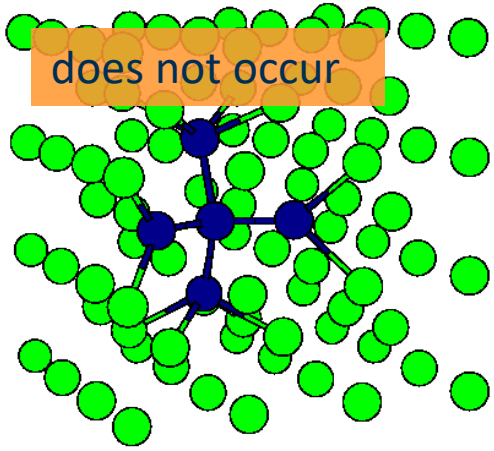

tetrahedral

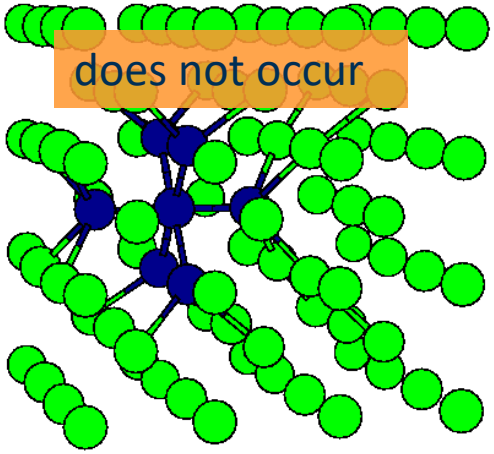

octahedral

Dynamics of self-interstitial defects

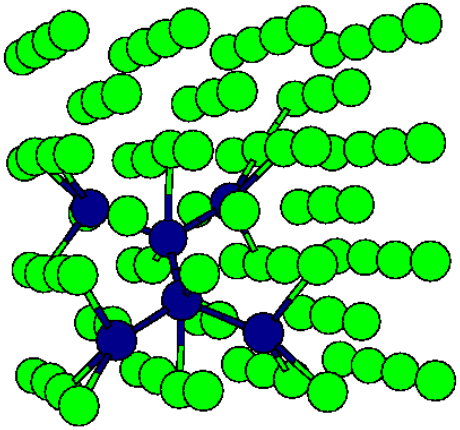

110 dumbbell

Thermal migration of a 110 dumbbell. Occurs in Fe and ferritic steels.

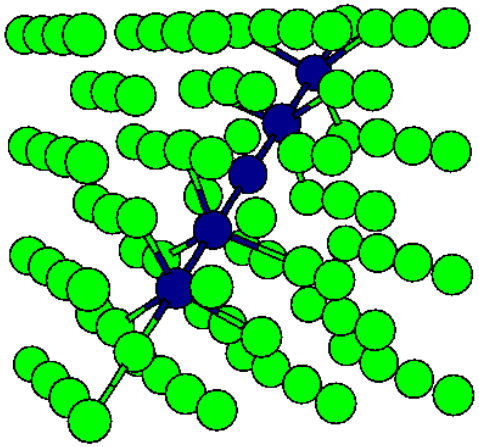

111 crowdion

Thermal migration of a linear 111 type defect. Occurs in non-magnetic transition metals (tungsten, vanadium, molybdenum).

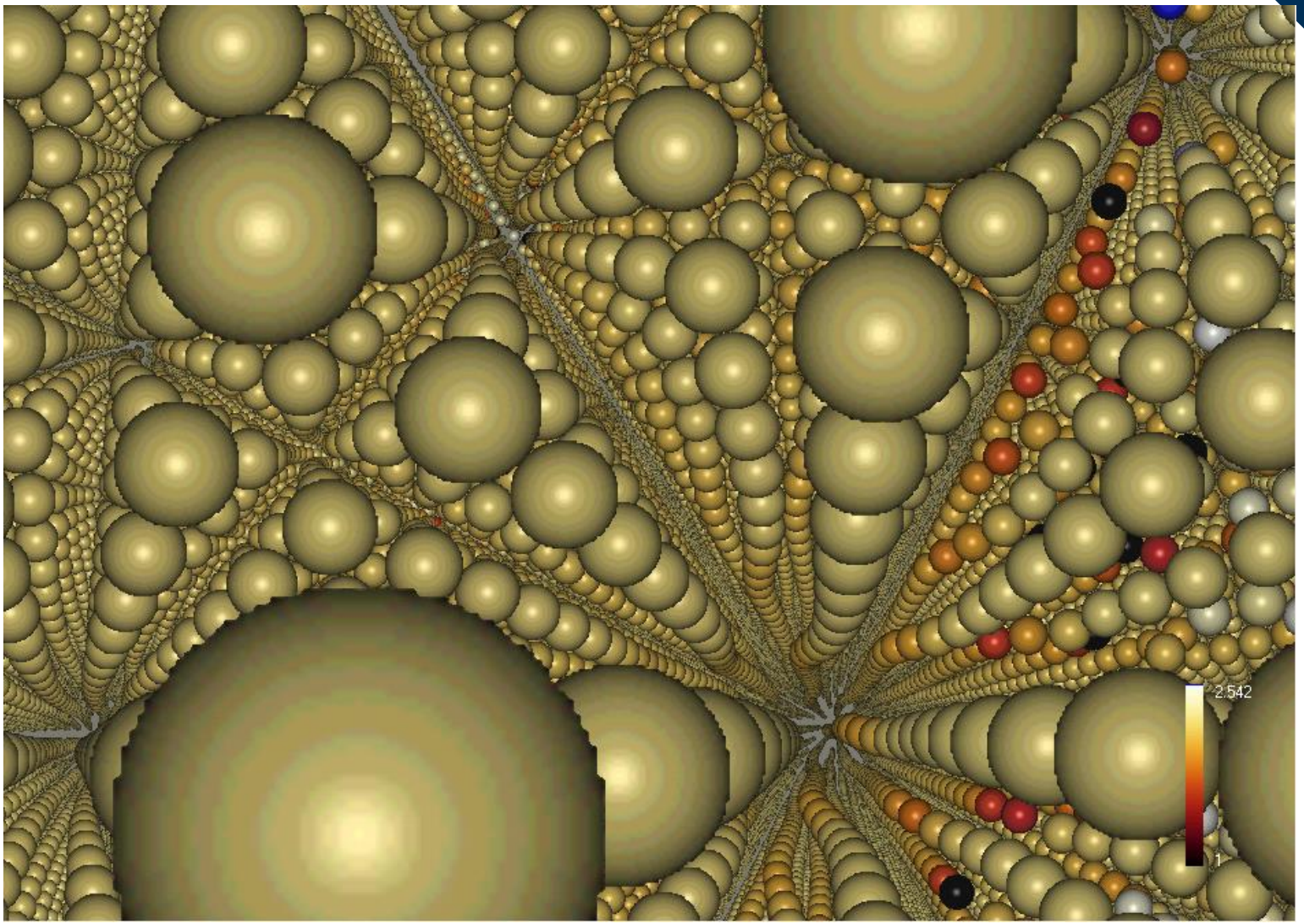

Lattice distortions are of primary significance to engineering, where they are known as “strains and stresses”.

Stress field produced by a cascade

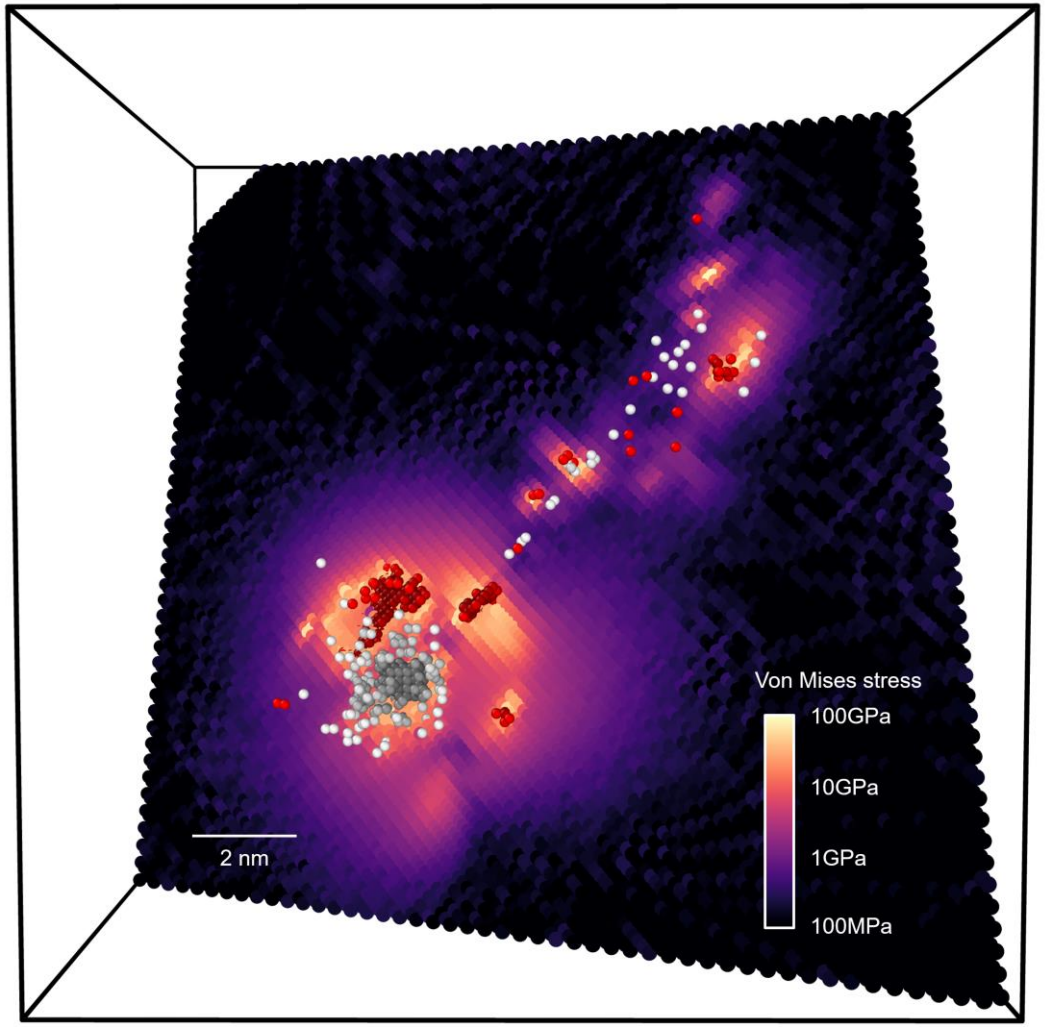

Stress field in the vicinity of defects formed in a collision cascade.

D. R. Mason *et al., Journ. Appl. Phys.* (2019) in press

Elastic fields of defects

$$u_i(\mathbf{r}) = -P_{kl}\frac{\partial}{\partial x_l}G_{ik}(\mathbf{r}-\mathbf{R})$$

$$G_{ik}(\mathbf{r}) = \frac{1}{16\pi\mu(1-\nu)r}\left[(3-4\nu)\delta_{ik} + \frac{x_i x_k}{r^2}\right]$$

Green's function of elasticity: the field of atomic displacements generated by a point source. Different from the Coulomb law because in a solid there are two different velocities of sound, longitudinal and transverse.

Elastic fields of defects

$$u_i(\mathbf{r}) = -P_{kl}\frac{\partial}{\partial x_l}G_{ik}(\mathbf{r}-\mathbf{R})$$

$$G_{ik}(\mathbf{r}) = \frac{1}{16\pi\mu(1-\nu)r}\left[(3-4\nu)\delta_{ik} + \frac{x_i x_k}{r^2}\right]$$

$$P_{kl} = \begin{pmatrix} P_{11} & P_{12} & P_{13} \\ P_{12} & P_{22} & P_{23} \\ P_{13} & P_{23} & P_{33} \end{pmatrix}$$

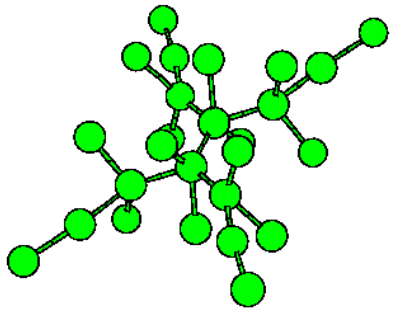

elastic dipole tensor – a 3x3 symmetric real matrix containing six independent parameters (three eigenvalues defining the shape of the defect, and three angles defining its orientation).

Elastic fields of defects

$$u_i(\mathbf{r}) = -P_{kl}\frac{\partial}{\partial x_l}G_{ik}(\mathbf{r}-\mathbf{R})$$

$$G_{ik}(\mathbf{r}) = \frac{1}{16\pi\mu(1-\nu)r}\left[(3-4\nu)\delta_{ik} + \frac{x_i x_k}{r^2}\right]$$

$$P_{kl} = -\int_V \sigma_{kl}(\mathbf{r})\mathrm{d}^3 r = -V\overline{\sigma}_{kl}$$

Amazingly, the elements of this tensor are almost always computed, by DFT or molecular statics, in any simulation involving atomic relaxations.

E. Clouet *et al.*, Acta Materialia 56 (2008) 3450;
P.-W. Ma and S.L. Dudarev, Phys. Rev. Mat. 3 (2019) 013605

Elastic fields of defects

$$u_i(\mathbf{r}) = -P_{kl}\frac{\partial}{\partial x_l}G_{ik}(\mathbf{r}-\mathbf{R})$$

$$G_{ik}(\mathbf{r}) = \frac{1}{16\pi\mu(1-\nu)r}\left[(3-4\nu)\delta_{ik} + \frac{x_i x_k}{r^2}\right]$$

$$P_{kl} = -\int_V \sigma_{kl}(\mathbf{r})\mathrm{d}^3 r = -V\overline{\sigma}_{kl}$$

$$P_{kl} = C_{klmn}\Omega_{mn}$$

relaxation volume tensor: the sum of its diagonal elements gives the relaxation volume of the defect

S.L. Dudarev *et al.*, Nucl. Fusion 58 (2018) 126002

Dipole and relaxation volume tensors

UK Atomic Energy Authority

TABLE XXIV. Elements of the dipole tensor P_{ij} (in eV units), the relaxation volume tensor Ω_{ij} (in Å^3 units), eigenvalues of the relaxation volume tensor $\Omega^{(i)}$ (in Å^3 units), and the relaxation volume of the defect $\Omega_{\rm rel}$ (in atomic volume units Ω_0) computed for Fe.

Fe	P_{11}	P_{22}	P_{33}	P_{12}	P_{23}	P_{31}	Ω_{11}	Ω_{22}	Ω_{33}	Ω_{12}	Ω_{23}	Ω_{31}	$\Omega^{(1)}$	$\Omega^{(2)}$	$\Omega^{(3)}$	$\Omega_{\rm rel}$
⟨111⟩d	23.465	23.465	23.472	5.850	5.851	5.851	6.327	6.327	6.335	4.362	4.363	4.363	1.964	1.964	15.051	1.673
⟨111⟩c	23.186	23.186	23.193	5.903	5.904	5.904	6.252	6.252	6.259	4.402	4.402	4.402	1.850	1.850	15.056	1.653
⟨110⟩d	25.832	21.143	21.150	0.000	5.122	0.000	9.777	4.294	4.302	0.000	3.819	0.000	9.777	0.475	8.122	1.620
Tetra	21.396	23.331	23.339	0.000	0.001	0.000	4.607	6.871	6.880	0.000	0.000	0.000	4.607	6.871	6.880	1.619
⟨100⟩d	32.284	22.931	22.937	0.000	0.000	0.000	14.316	3.378	3.385	0.000	0.000	0.000	14.316	3.378	3.385	1.858
Octa	23.273	23.273	31.302	0.000	0.000	0.000	3.869	3.869	13.258	0.000	0.000	0.000	3.869	3.869	13.258	1.851
Vac	−3.081	−3.081	−3.081	0.000	0.000	0.000	−0.831	−0.831	−0.831	0.000	0.000	0.000	−0.831	−0.831	−0.831	−0.220

TABLE XX. Elements of the dipole tensor P_{ij} (in eV units), the relaxation volume tensor Ω_{ij} (in Å^3 units), eigenvalues of the relaxation volume tensor $\Omega^{(i)}$ (in Å^3 units), and the relaxation volume of the defect $\Omega_{\rm rel}$ (in atomic volume units Ω_0) computed for W.

W	P_{11}	P_{22}	P_{33}	P_{12}	P_{23}	P_{31}	Ω_{11}	Ω_{22}	Ω_{33}	Ω_{12}	Ω_{23}	Ω_{31}	$\Omega^{(1)}$	$\Omega^{(2)}$	$\Omega^{(3)}$	$\Omega_{\rm rel}$
⟨111⟩d	52.754	52.754	52.754	13.128	13.128	13.128	9.209	9.209	9.209	7.402	7.402	7.402	1.808	1.808	24.012	1.712
⟨111⟩c	52.745	52.745	52.745	13.151	13.151	13.151	9.207	9.207	9.207	7.414	7.414	7.414	1.793	1.793	24.036	1.711
⟨110⟩d	56.960	52.557	52.557	0.000	11.277	0.000	10.908	8.693	8.693	0.000	6.358	0.000	10.908	2.335	15.050	1.753
Tetra	47.359	59.114	59.114	0.000	0.000	0.000	5.693	11.606	11.606	0.000	0.000	0.000	5.693	11.606	11.606	1.791
⟨100⟩d	65.920	53.379	53.379	0.000	0.000	0.000	14.254	7.945	7.945	0.000	0.000	0.000	14.254	7.945	7.945	1.868
Octa	52.741	52.741	67.209	0.000	0.000	0.000	7.623	7.623	14.901	0.000	0.000	0.000	7.623	7.623	14.901	1.868
Vac	−9.984	−9.984	−9.984	0.000	0.000	0.000	−1.743	−1.743	−1.743	0.000	0.000	0.000	−1.743	−1.743	−1.743	−0.324

P.-W. Ma and S.L. Dudarev, Phys. Rev. Mat. **3** (2019) 013605

Elastic fields of defects

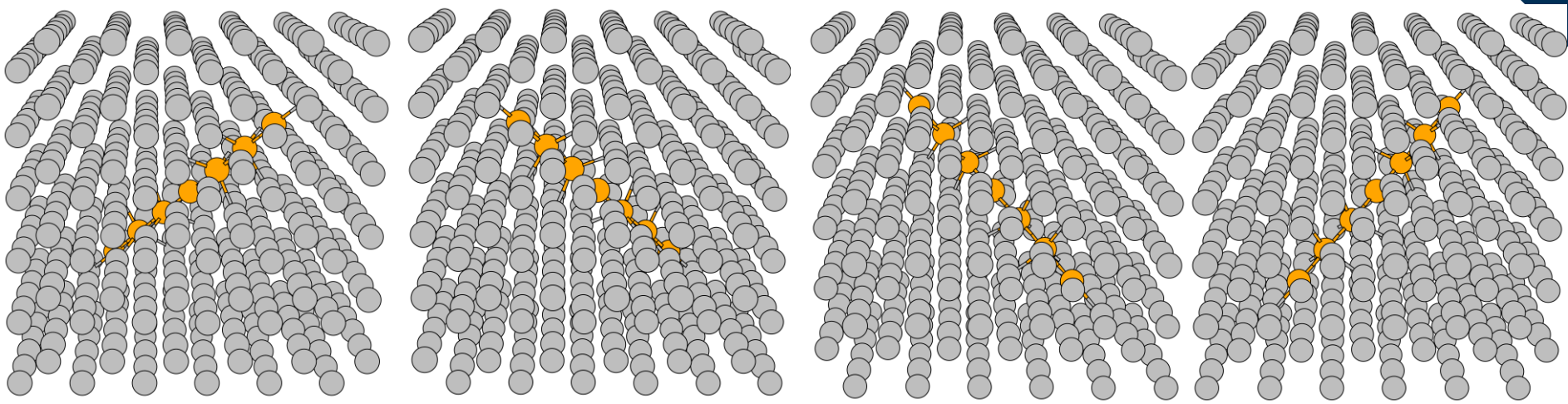

$$\begin{pmatrix} P_a & P_b & P_b \\ P_b & P_a & P_b \\ P_b & P_b & P_a \end{pmatrix} \quad \begin{pmatrix} P_a & -P_b & P_b \\ -P_b & P_a & -P_b \\ P_b & -P_b & P_a \end{pmatrix} \quad \begin{pmatrix} P_a & P_b & -P_b \\ P_b & P_a & -P_b \\ -P_b & -P_b & P_a \end{pmatrix} \quad \begin{pmatrix} P_a & -P_b & -P_b \\ -P_b & P_a & P_b \\ -P_b & P_b & P_a \end{pmatrix}$$

Averaging over orientations produces a diagonal tensor

$$\begin{pmatrix} P_a & 0 & 0 \\ 0 & P_a & 0 \\ 0 & 0 & P_a \end{pmatrix} = P_a \delta_{ij}$$

Strain field of defects

In applications, we are interested in the elastic field produced by many defects => self-averaging

$$\langle \Omega_{mn} \rangle = \sum_{s=1}^{3} \Omega^{(s)} \langle e_m^{(s)} e_n^{(s)} \rangle$$

$$\langle \Omega_{mn} \rangle = \frac{1}{3} \Omega_{\mathrm{rel}} \delta_{mn}$$

Anisotropic crystallographic effects are also not significant for large structural components where the orientations of grains are random

strain

$$\epsilon_{ij}(\mathbf{r}) = \frac{1}{4\pi} \frac{1+\nu}{1-\nu} \int \frac{\omega_{\mathrm{rel}}(\mathbf{R})}{|\mathbf{r}-\mathbf{R}|^3} \left(\frac{1}{3}\delta_{ij} - \eta_i \eta_j \right) \mathrm{d}^3 R \qquad \eta_i = \frac{(\mathbf{r}-\mathbf{R})_i}{|\mathbf{r}-\mathbf{R}|}$$

$$\omega_{\mathrm{rel}}(\mathbf{r}) = \sum_a \Omega_{\mathrm{rel}}^{(a)} \delta(\mathbf{r} - \mathbf{R}_\alpha)$$

dimensionless

$\omega(\mathbf{r})$ is the density of relaxation volumes of defects.

Stress field of defects

The next (key) step: computing stresses.

$$\eta_i = \frac{(\mathbf{r}-\mathbf{R})_i}{|\mathbf{r}-\mathbf{R}|}$$

$$\epsilon_{ij}(\mathbf{r}) = \frac{1}{4\pi}\frac{1+\nu}{1-\nu}\int \frac{\omega_{\mathrm{rel}}(\mathbf{R})}{|\mathbf{r}-\mathbf{R}|^3}\left(\frac{1}{3}\delta_{ij} - \eta_i\eta_j\right)\mathrm{d}^3R$$

Strain tensor does not enter the equilibrium conditions and not convenient in the context of FEM. Computing stresses requires convoluting the strain tensor with the tensor of elastic constants:

$$\sigma_{ij}(\mathbf{r}) = C_{ijkl}\epsilon_{kl}(\mathbf{r}) \qquad C_{ijkl} = \mu\frac{2\nu}{1-2\nu}\delta_{ij}\delta_{kl} + \mu\left(\delta_{ik}\delta_{jl} + \delta_{il}\delta_{jk}\right)$$

$$\sigma_{ij}(\mathbf{r}) = -\frac{\mu}{6\pi}\frac{1+\nu}{1-\nu}\int \omega_{\mathrm{rel}}(\mathbf{R})\frac{\partial^2}{\partial x_i \partial x_j}\frac{1}{|\mathbf{r}-\mathbf{R}|}\mathrm{d}^3R \longleftarrow \text{non-local}$$

$$+\frac{\mu}{3}\left(\frac{1+\nu}{1-\nu}\right)\left(\frac{2\nu}{1-2\nu}\right)\delta_{ij}\omega_{\mathrm{rel}}(\mathbf{r}). \longleftarrow \text{local}$$

S.L. Dudarev *et al.*, Nucl. Fusion 58 (2018) 126002

Stress field of defects

$$\sigma_{ij}(\mathbf{r}) = -\frac{\mu}{6\pi}\frac{1+\nu}{1-\nu}\int \omega_{\mathrm{rel}}(\mathbf{R})\frac{\partial^2}{\partial x_i \partial x_j}\frac{1}{|\mathbf{r}-\mathbf{R}|}\mathrm{d}^3R + \frac{\mu}{3}\left(\frac{1+\nu}{1-\nu}\right)\left(\frac{2\nu}{1-2\nu}\right)\delta_{ij}\omega_{\mathrm{rel}}(\mathbf{r}).$$

Using this, it is possible to compute the *derivative* of stress – which is known as the "body force"

$$\frac{\partial \sigma_{ik}}{\partial x_k} = \frac{2\mu}{3}\left(\frac{1+\nu}{1-2\nu}\right)\frac{\partial}{\partial x_i}\omega_{rel}(\mathbf{r}) = B\frac{\partial}{\partial x_i}\omega_{rel}(\mathbf{r})$$

B is the bulk modulus of the material.

S.L. Dudarev *et al.*, Nucl. Fusion 58 (2018) 126002

Condition of global equilibrium

Condition of equilibrium includes gravity, thermal expansion, *and* swelling due to defects

$$\frac{\partial \sigma_{ik}(\mathbf{r})}{\partial x_k} + \rho g_i - B\alpha \frac{\partial T}{\partial x_i} - B \frac{\partial}{\partial x_i} \omega_{rel}(\mathbf{r}) = 0.$$

gravity

thermal expansion

defects

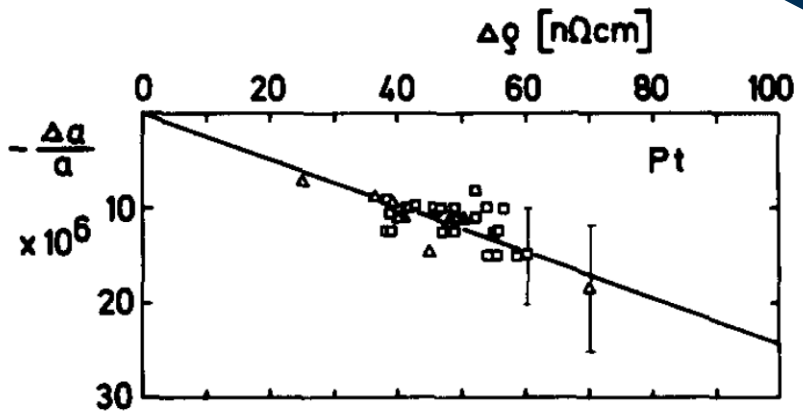

Fig. 1. Lattice parameter versus resistivity change after quenching of Pt. (Δ(333/511), □ (422) X-ray reflection).

$$\left(\frac{\Delta v}{v}\Big/\Delta\rho\right)_v^{Pt} = -(0.72 \pm 0.09) \times 10^3\ (\Omega\,\mathrm{cm})^{-1}$$

Defects, as opposed to temperature, generate compressive or tensile strains: this agrees with DFT

W. Hertz et al., Phys. Letters **43A** (1973) 289

A finite element model implementation

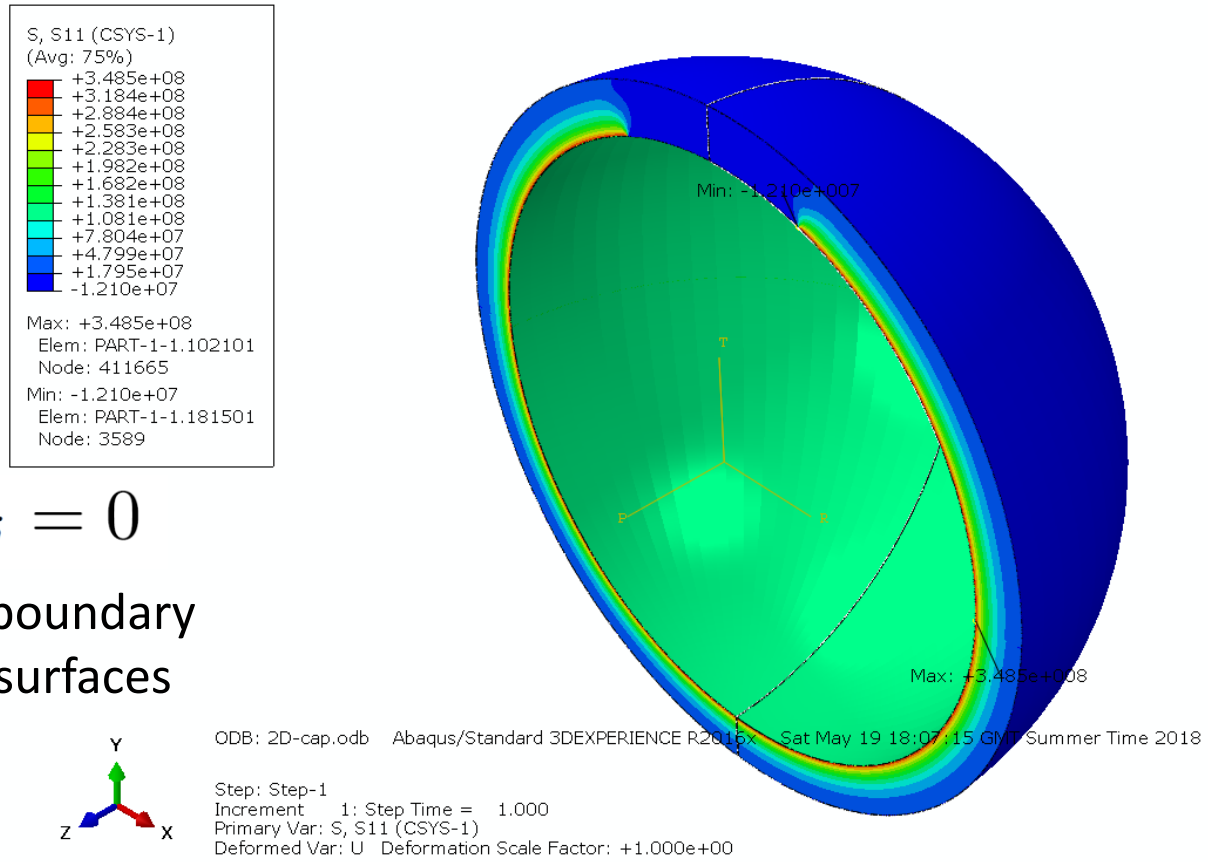

$$\sigma_{ij}(\mathbf{r})n_j = 0$$

Traction free boundary conditions at surfaces

New equations have been implemented in the ABACUS finite element code. The FEM implementation also includes the various conventional body and surface forces, for example applied external stresses.

Nucl. Fusion **58** (2018) 126002

Case studies: a R=3m steel shell

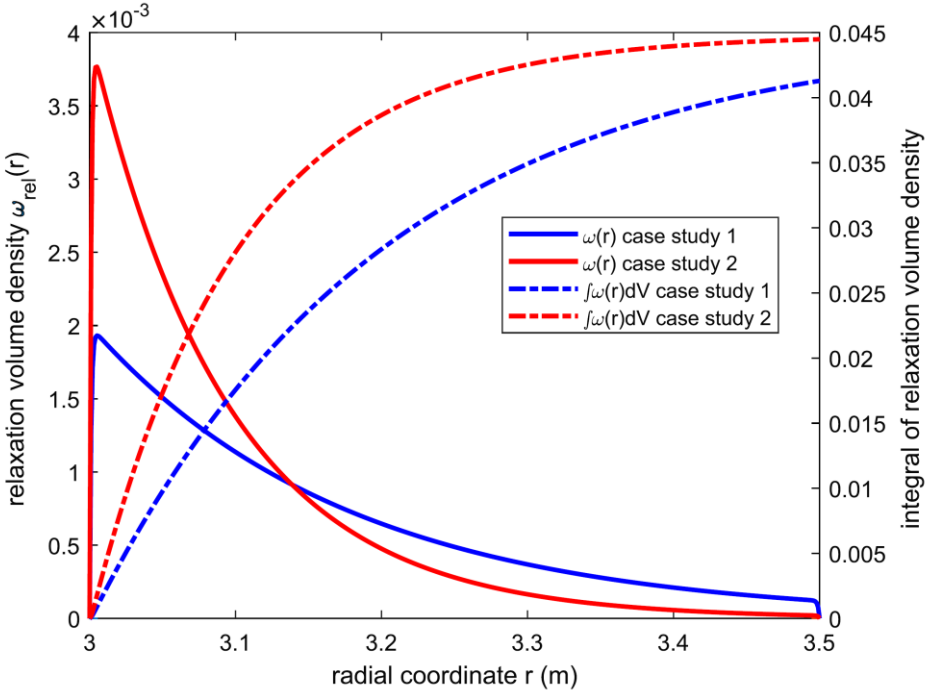

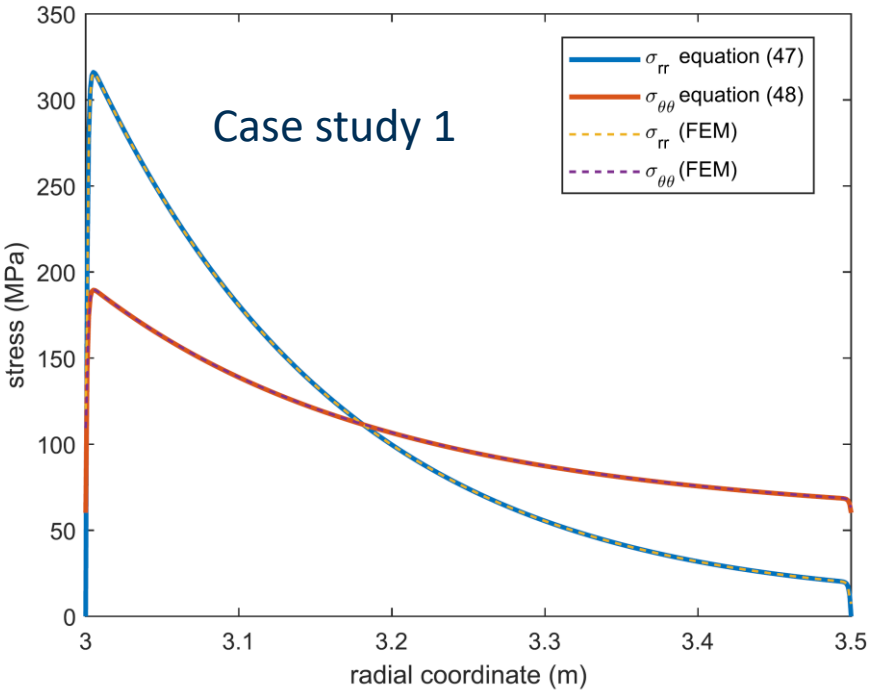

Analytical solutions of the equilibrium elasticity equations and numerical finite element solutions agree exactly. High stresses develop even if swelling is low.

$$\sigma_{\theta\theta}(r) = \frac{\mu}{3\pi}\left(\frac{1+\nu}{1-\nu}\right)\left[\frac{\Omega_{\text{tot}}}{R_2^3 - R_1^3}\left(1+\frac{R_1^3}{2r^3}\right)\right] + \frac{\mu}{6\pi}\left(\frac{1+\nu}{1-\nu}\right)\left[\frac{4\pi}{r^3}\int_{R_1}^{r} R^2\omega_{\text{rel}}(R)\,\mathrm{d}R\right] + \frac{\mu}{3}\left(\frac{1+\nu}{1-\nu}\right)\left(\frac{2\nu}{1-2\nu}\right)\omega_{\text{rel}}(r).$$

Nucl. Fusion **58** (2018) 126002

Statistics of generation of defects

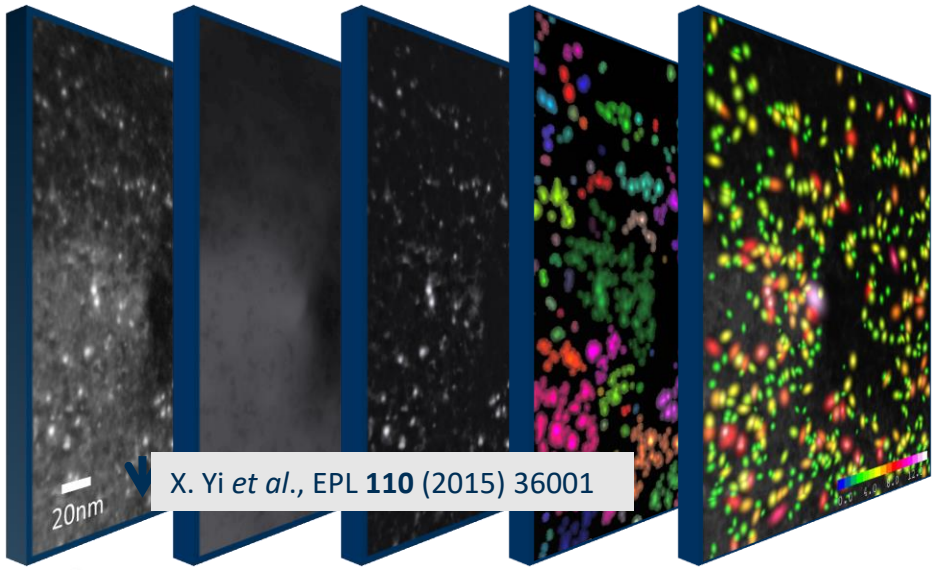

X. Yi *et al.*, EPL **110** (2015) 36001

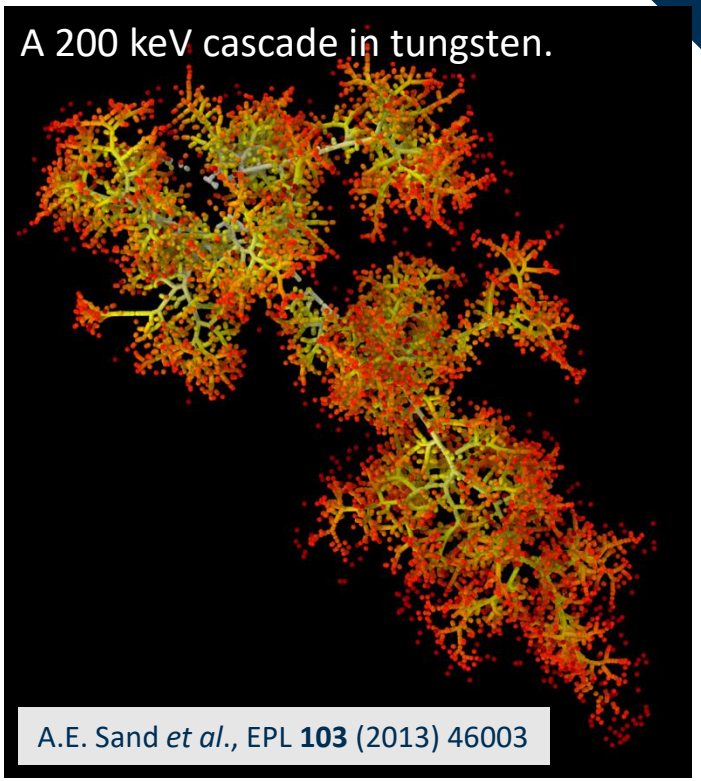

A.E. Sand *et al.*, EPL **103** (2013) 46003

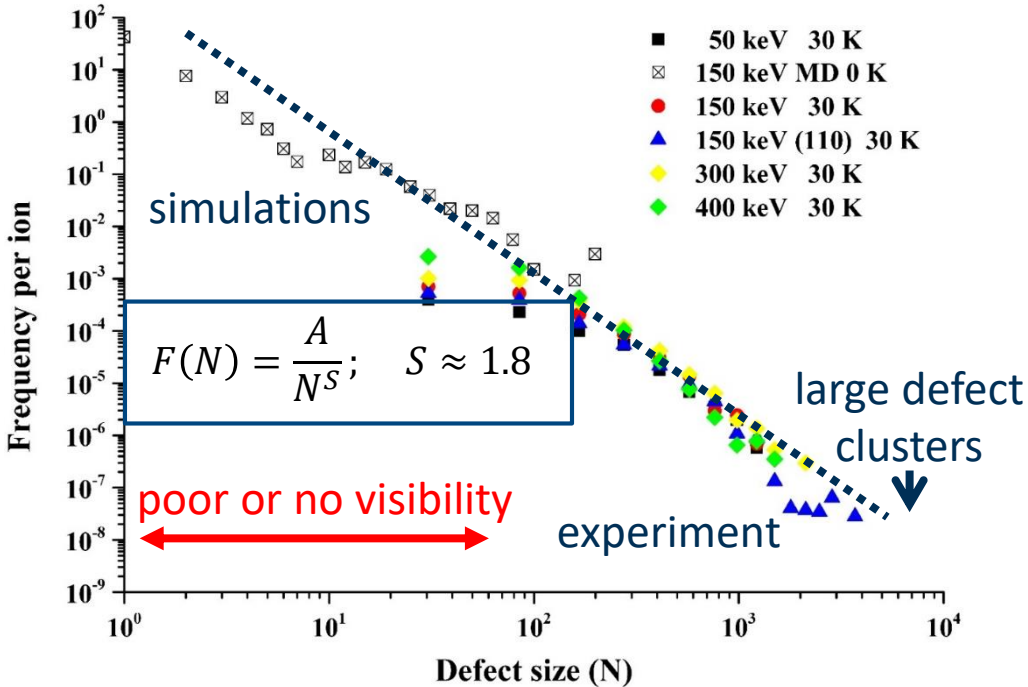

Analysis of hundreds of collision cascade simulations, and tens of thousand of events recorded in electron microscope images shows that the statistics of sizes of defect clusters follow a power law – like earthquakes or avalanches.

Relaxation volumes of complex defects

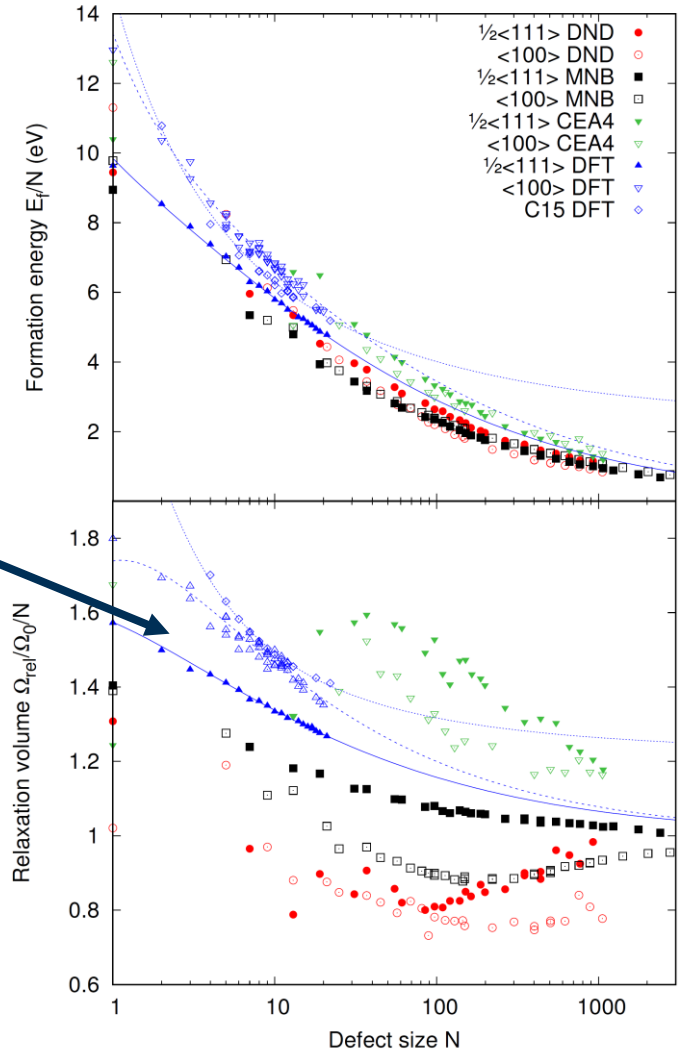

Interstitial loops

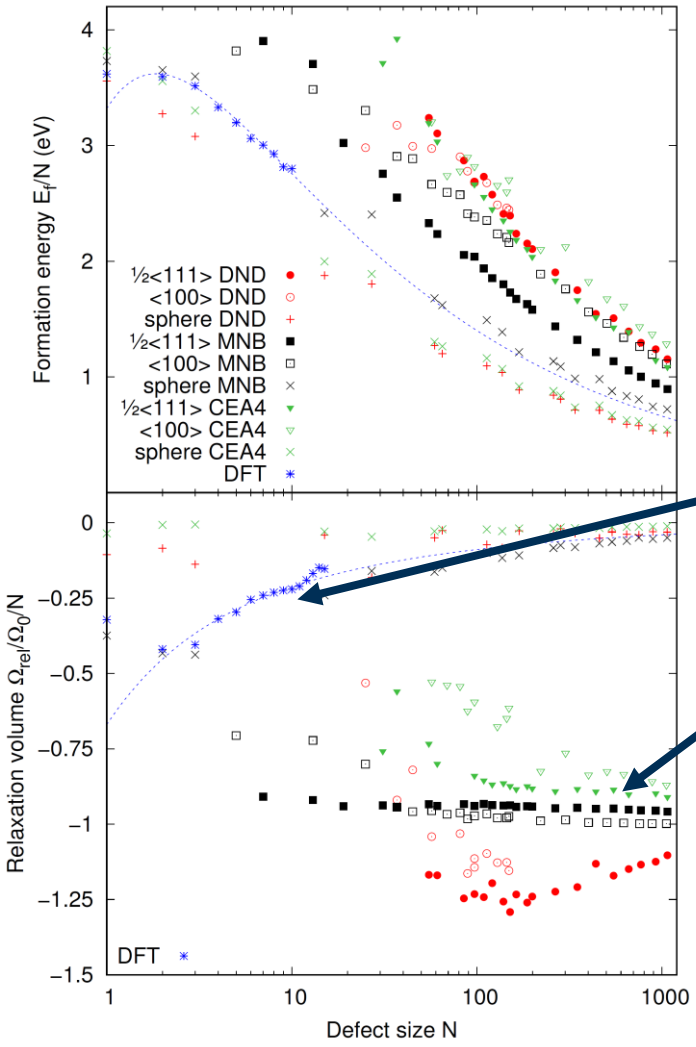

Voids

Vacancy loops

This spans the poor or no visibility size range.

D. R. Mason *et al., Journ. Appl. Phys.* (2019) in press

Relaxation volume of a dislocation loop

$$P_{ij} = \mu \left[(b_i A_j + A_i b_j) + \frac{2\nu}{1-2\nu} (\boldsymbol{b} \cdot \boldsymbol{A}) \delta_{ij} \right] . \quad \mathbf{A} = \frac{1}{2} \oint (\mathbf{r} \times d\mathbf{l})$$

$$\Omega_{rel} = (\mathbf{b} \cdot \mathbf{A}) = \frac{1}{2} \oint \mathbf{b} \cdot (\mathbf{r} \times d\mathbf{l})$$

← independent of the distance to the surface

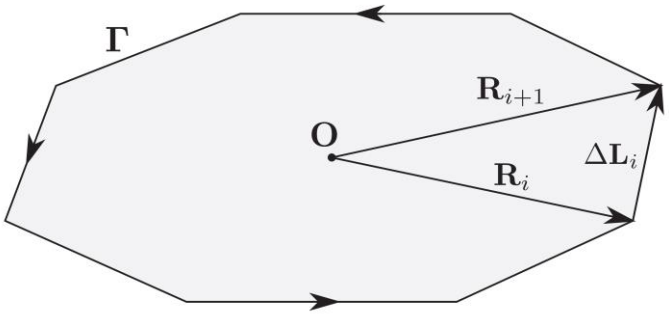

FIG. 13. Sketch of the vectors $\mathbf{R}_i$, $\mathbf{R}_{i+1}$, and $\Delta\mathbf{L}_i$ with respect to the boundary Γ of the dislocation loop. The arrows on Γ denote the direction of the dislocation line.

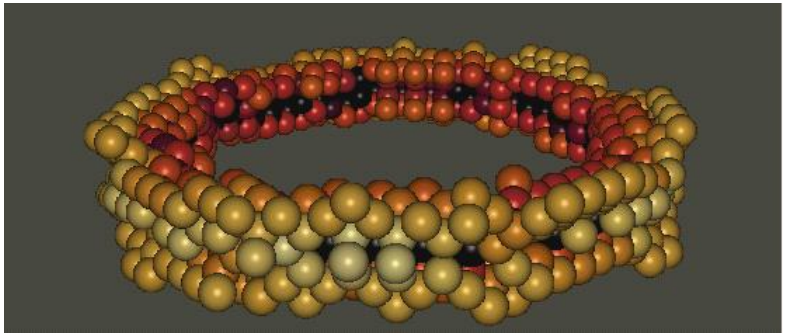

The relaxation volume of a dislocation loop equals the volume of the same number of atoms as the number of defects forming the loop. Can be positive or negative (SIA or vacancy). Invariant if the loop glides.

I. Rovelli *et al.,* Phys. Rev. E **98** (2018) 043002; S.L. Dudarev and P.-W. Ma, Phys. Rev. Materials **2** (2018) 033602

Relaxation volume of a helium bubble

$$\Omega_{rel} = \frac{\pi a^3 \left(p_a - 2\gamma/a\right)\left(3K + 4\mu\right)}{3K\mu}$$
$$= \frac{3\pi a^3}{\mu}\left(\frac{1-\nu}{1+\nu}\right)\left(p_a - \frac{2\gamma}{a}\right)$$

p is the pressure of gas inside the bubble and *γ* is the average surface energy density. If *p=0*, the relaxation volume of a void is:

$$\Omega_{rel} \simeq -6\pi\left(\frac{1-\nu}{1+\nu}\right)\frac{\gamma a^2}{\mu}$$

It is negative - hence material containing only voids and no dislocation loops, contracts.

D. R. Mason *et al., Journ. Appl. Phys.* (2019) in press

Microstructure driven by elastic forces

UK Atomic Energy Authority

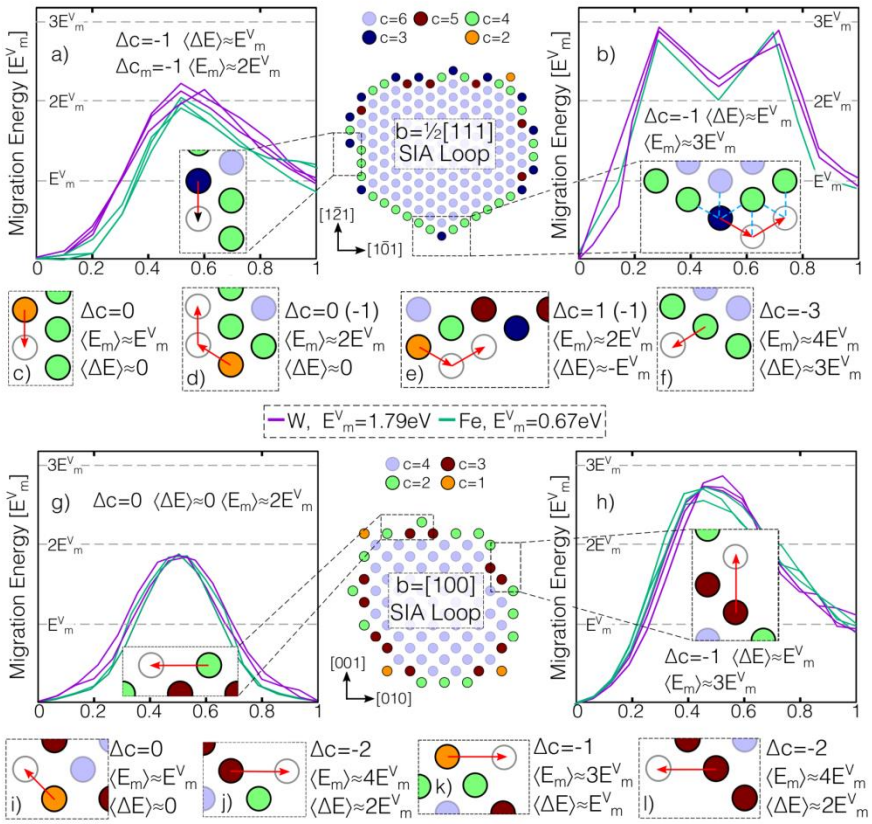

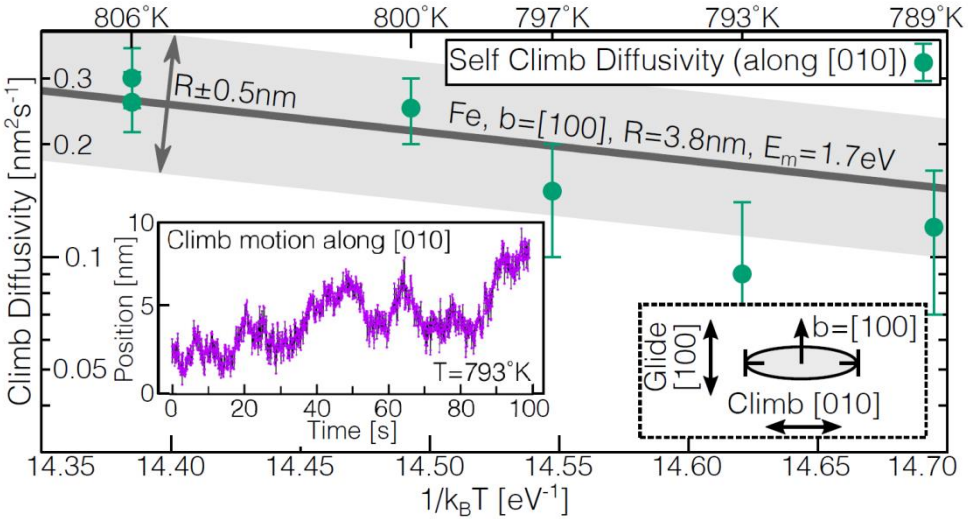

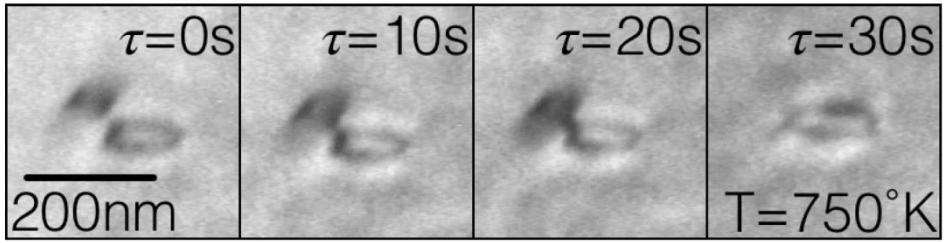

	R_1[nm]	R_2[nm]	d[nm]	T[K]	τ_{exp}[s]	τ_{SC}[s]	τ_{VMC}[s]
Fe	150	30	70	750	30.0	50.2	3.3×10^{7}
Fe	3.5	3.5	7	660	~0.8	1.8	2.7×10^{7}
Fe[§]	~5.	~5.	~10.	725	~6.	2.1	2.7×10^{7}
W[†]	20	20	100	1173	66.5	96.2	2.6×10^{7}
W[†]	100	500*	100	1273	7.	8.6	1.5×10^{5}

Dislocation climb may occur due to the diffusion of atoms around the perimeter of a dislocation loop, independent of the vacancy atmosphere. At low temperatures this self-climb is orders of magnitude faster than vacancy-diffusion-mediated climb.

T. D. Swinburne *et al., Sci. Repts.* **6** (2016) 30596

Stochastic dislocation dynamics

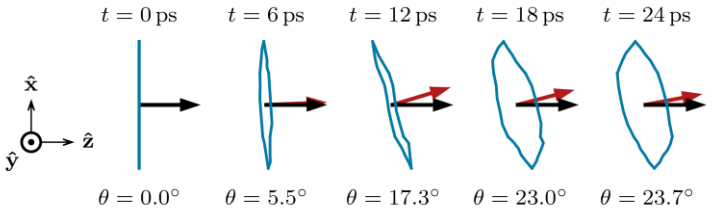

a) stochastic dislocation dynamics snapshots

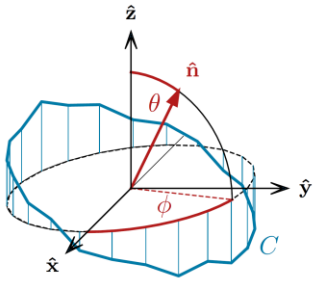

b) habit plane angles θ and ϕ

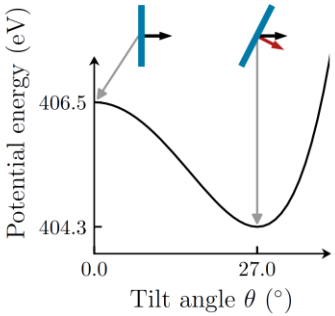

c) energy versus tilt angle θ

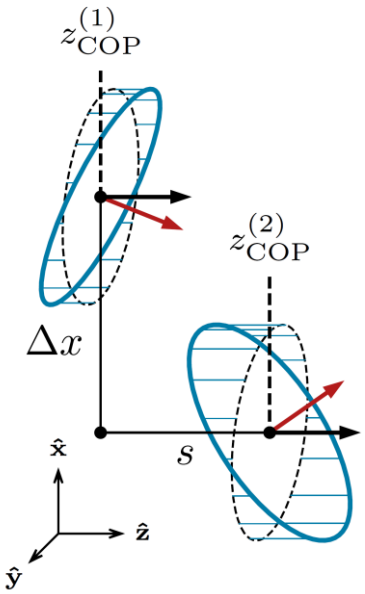

a) Two interacting loops

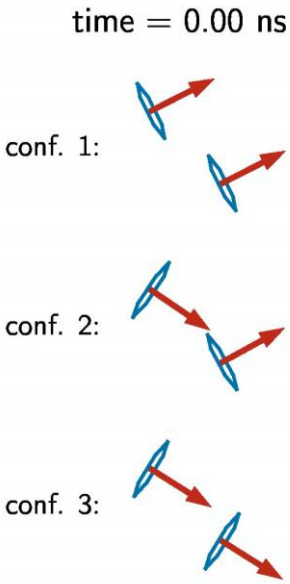

TABLE II. The lifetime of an elastically confined pair of dislocation loops computed for some selected loop radii ρ and temperatures T assuming the separation between the loops in a plane perpendicular to their glide cylinders of $\Delta x = 12$ nm. Three distinct configurations of pairs of loops are considered.

Conditions	Pure prismatic	Lowest PES	30° fixed tilt
$\rho = 4.5$ nm, $T = 200$ K	$\sim 10^{259}$ yr	$\sim 10^{258}$ yr	$+\infty$
$\rho = 4.5$ nm, $T = 600$ K	$\sim 10^{75}$ yr	$\sim 10^{75}$ yr	$\sim 10^{117}$ yr
$\rho = 2.0$ nm, $T = 200$ K	4 s	18 min	3 yr
$\rho = 2.0$ nm, $T = 300$ K	5 µs	0.3 s	5 min
$\rho = 2.0$ nm, $T = 400$ K	0.2 ms	6 ms	0.5 s
$\rho = 2.0$ nm, $T = 500$ K	0.02 ms	0.5 ms	10 ms
$\rho = 2.0$ nm, $T = 600$ K	0.005 ms	0.1 ms	0.8 ms

Y. Li, M. Boleininger, C. Robertson *et al.* (2019)

Recovery of microstructure

Including effects of surfaces requires using Kinchoff's formula relating derivatives of Green's functions in the volume of the material and at surfaces, to fully define the field of vacancies everywhere in the sample

$$\int_V dV' \left[c(\mathbf{x}') \frac{\partial^2 G_0(\mathbf{x},\mathbf{x}')}{\partial \mathbf{x}'^2} - G_0(\mathbf{x},\mathbf{x}') \frac{\partial^2 c(\mathbf{x}')}{\partial \mathbf{x}'^2} \right] = \int_S dS' \left[c(\mathbf{x}') \left(\mathbf{n} \cdot \frac{\partial G_0(\mathbf{x},\mathbf{x}')}{\partial \mathbf{x}'} \right) - G_0(\mathbf{x},\mathbf{x}') \left(\mathbf{n} \cdot \frac{\partial c(\mathbf{x}')}{\partial \mathbf{x}'} \right) \right]$$

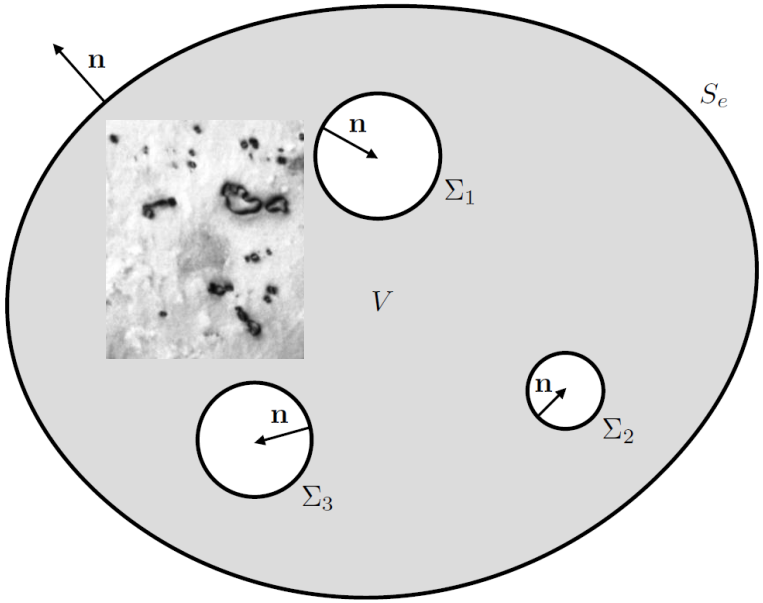

In the right-hand side of this equation, vacancy concentration at a point **x**' at a surface can be evaluated just like at dislocation lines.

Evaporation of vacancies from dislocations is driven by elastic self-stress. At surfaces, evaporation is driven by surface tension.

A system of coupled ODEs for the velocities of nodes on dislocation lines and at surfaces. The dynamics of diffusion-mediated evolution of dislocations and cavities/surfaces is fully defined.

I. Rovelli *et al., Journ. Mech. Phys. Solids* **103** (2017) 121

Recovery of microstructure

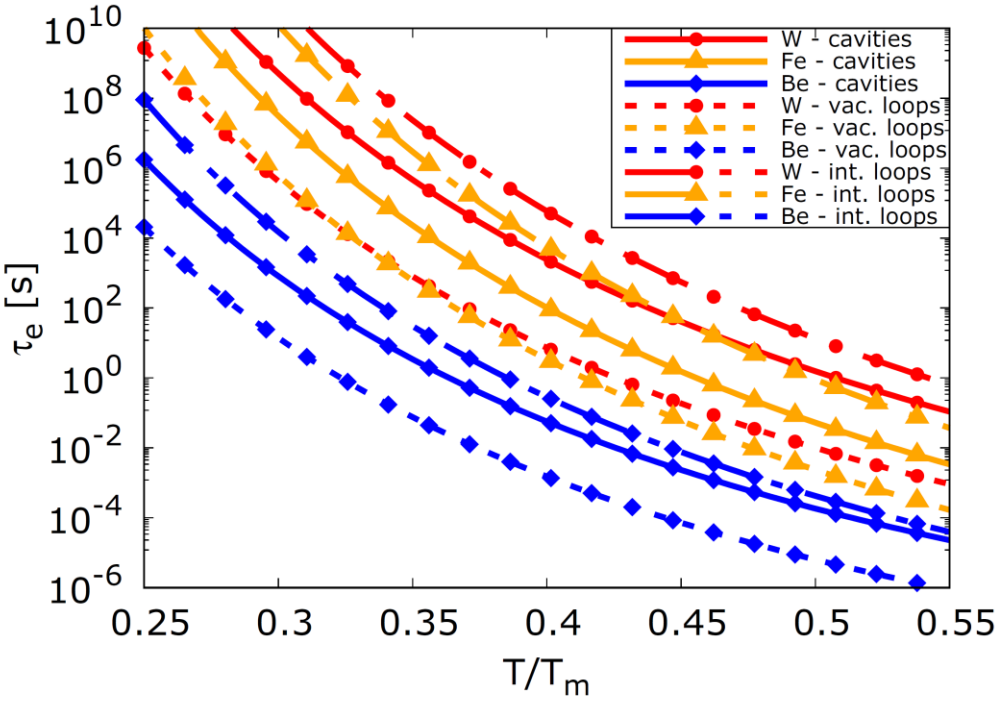

Estimated timescales for the evaporation of vacancy dislocation loops, vacancy clusters (voids) and self-interstitial loops in Be, Fe and W at various temperatures. Note the high temperature sensitivity of the estimated values.

I. Rovelli *et al., Physical Review* **E98** (2018) 043002

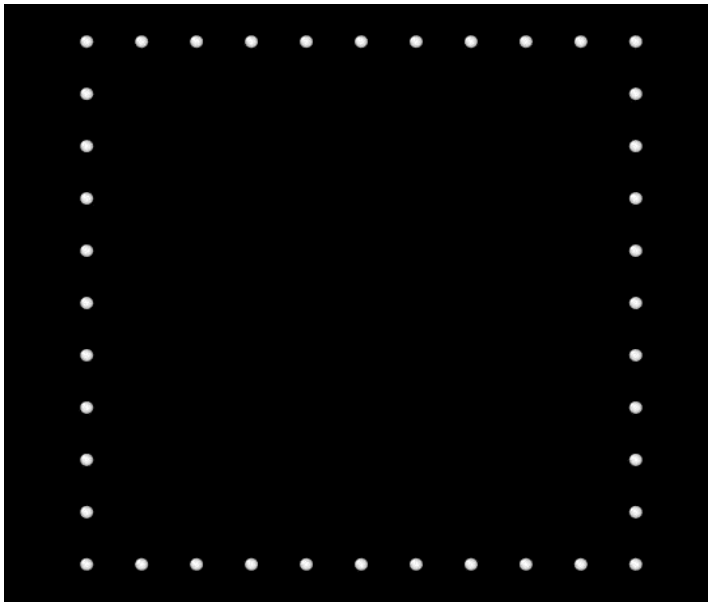

Vacancy loop in tungsten, evaporating due to its own self-stress at T~1600 C. Initial size of the loop is 100 A, the total evaporation time is ~10 s.

A. Breidi *et al*. (2019)

Summary

$$\frac{\partial \sigma_{ik}(\mathbf{r})}{\partial x_k} + \rho g_i - B\alpha \frac{\partial T}{\partial x_i} - B \frac{\partial}{\partial x_i} \omega_{rel}(\mathbf{r}) = 0.$$

A fundamental condition of elastic equilibrium, containing no free parameters, and including effects of gravity, thermal expansion and swelling due to defects.

Macroscopically, accumulation of defect produce body forces similar to thermal expansion, but the effect can be positive or negative. Note that the accumulation of defects itself depends on temperature.

Relaxation volumes of defects (the third term) includes invisible defects and can be computed numerically (DFT or MD). There are also analytical formulae for the relaxation volume of a dislocation loop, a void or a gas bubble.